Programmable femtosecond pulse shaping by use of a multielement liquid-crystal phase modulator

A. M. Weiner, D. E. Leaird, J. S. Patel, and J. R. Wullert

Bellcore, 331 Newman Springs Road, Red Bank, New Jersey 07701-7040

Received November 27, 1989; accepted January 8, 1990

We report programmable shaping of femtosecond optical pulses by use of a multielement liquid-crystal modulator to manipulate the phases of spatially dispersed optical frequency components. Our approach provides for continuously variable control of the optical phase and permits the pulse shape to be reconfigured on a millisecond time scale. We use the apparatus to demonstrate femtosecond pulse-position modulation as well as programmable compression of chirped femtosecond pulses.

Considerable effort has been directed toward generating ever shorter optical pulses, and pulses as short as 6 fsec are now available.[1] More recently, interest in synthesis of ultrashort pulses with arbitrarily controllable pulse shapes[2–6] has also arisen. Specially shaped ultrashort pulses are now being used to study high-speed optical communications,[4] nonlinear optics in fibers,[7–9] and time-resolved spectroscopy.[8,10]

Despite these successes, pulse-shaping techniques still suffer significant limitations. In particular, it has not been possible to achieve both high resolution[4] and electronic programmability[5] at the same time (although both attributes have been demonstrated separately). In this Letter we describe a programmable, high-resolution, femtosecond pulse-shaping apparatus based on a multielement liquid-crystal phase modulator. We utilize our apparatus to achieve femtosecond pulse-position modulation and programmable femtosecond pulse compression.

Our pulse-shaping apparatus (Fig. 1) consists of a pair of 1800-line/mm gratings, placed at the focal planes of a unit-magnification confocal lens pair, and a 32-element liquid-crystal phase modulator. Except for the modulator, the apparatus is similar to our previous setups.[4,7,9,10] A colliding-pulse mode-locked ring dye laser[11] provides 75-fsec, 0.62-μm input pulses for the experiments. The first grating and lens spatially disperse the optical frequency spectrum of the input pulse. The multielement modulator is inserted midway between the lenses, where optimum spatial separation occurs. The second lens and grating recombine the various frequencies into a single collimated output beam, with the pulse shape given by the Fourier transform of the spectrum as modified by the phase modulator. The intensity profiles of the shaped pulses are measured by cross correlation, with pulses directly from the laser used as the probe. We note that our apparatus contributes no group-velocity dispersion; when the modulator is inactive, the output pulse is identical to the input.[2,4]

Our modulator consists of a 4-μm layer of nematic liquid crystal (British Drug House type E7) between two glass slides. The inner surfaces of the slides are coated with transparent indium tin oxide (ITO) conducting films. The ITO on one of the slides is patterned into a linear array of 32 independent electrodes spaced on 100-μm centers. The individual electrodes are separated by 5-μm gaps where the ITO is removed. The ITO on the other slide is left intact as a ground plane. An opaque metal film is deposited over a portion of the ground plane in order to define the 3.2-mm-wide optically active area.

The modulator operates as follows.[12] With no voltage applied, the liquid-crystal molecules are aligned with their longitudinal axis parallel to the polarization vector of the incident beam. At high voltages the liquid-crystal molecules tend to rotate so that their longitudinal axis is parallel to the applied field (i.e., in the direction of the beam path). The induced refractive-index change increases with the mean degree of rotation. With the ability to control independently and continuously the voltage applied to each electrode (or pixel), the device becomes a continuously variable (gray-level) phase modulator.

To demonstrate real-time pulse shaping, we performed a simple test in which each electrode was connected to either of two drive signals (D_1 and D_2) by means of 32 mechanical switches. D_1 was a 1-kHz square wave with zero mean and amplitude V_1; D_2 was switched at a 20-Hz rate between square waves of amplitudes V_1 and V_2. The more rapid (1-kHz) mod-

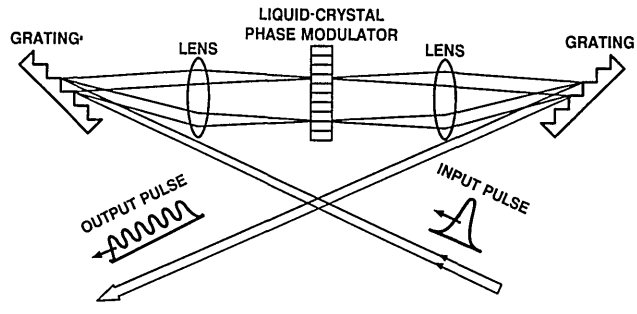

Fig. 1. Programmable femtosecond pulse-shaping apparatus. The lenses have a 15-cm focal length and are spaced by 30 cm. The 1800-line/mm gratings are placed at the focal planes of the lenses.

0146-9592/90/060326-03$2.00/0

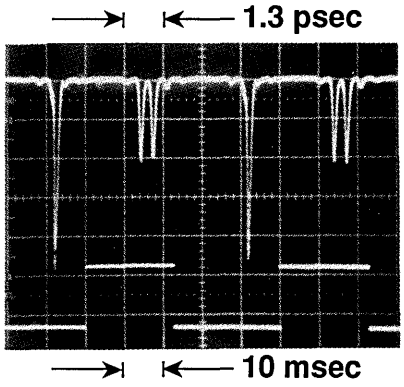

Fig. 2. Real-time pulse-shaping operation. Top trace: cross-correlation trace of the shaped pulses. Bottom trace: modulated drive signal (D_2) switching between V_1 = 1.9 V and V_2 = 5.0 V at a 20-Hz rate. The other drive signal (D_1, not shown) is kept at a constant 1.9-V level. The switches are set so that when D_2 is at 5.0 V, the phases are given by $\{0000\pi\pi\pi\pi0000\pi\pi\pi\pi0000\pi\pi\pi\pi0000\pi\pi\pi\pi\}$, resulting in a pulse doublet. When both drives are at 1.9 V, all the phases are the same, and a single pulse results.

ulation does not directly affect the phase but is required to prevent electromigration effects. When both D_1 and D_2 are set to amplitude V_1, all the pixels have the same phase, and no pulse shaping occurs. With two distinct amplitudes, however, different pixels have different phases (determined by the switch settings), and pulse reshaping is obtained. Figure 2 shows data obtained for a phase difference of π. The pulse intensity profiles are measured by using a real-time cross correlator synchronized to drive signal D_2. The data demonstrate complete switching from a single pulse to a pulse doublet within 25 msec. The actual turn-on and turn-off times measured at these bias levels are 2 and 20 msec, respectively.

In order to use our device as a gray-level phase modulator, we first calibrated its phase response. An amplitude mask, totally opaque except for two 100-μm clear apertures spaced 800 μm apart, was positioned adjacent to the modulator with the clear apertures aligned precisely with two modulator pixels. The two frequency components transmitted by the amplitude mask interfere to form a temporally modulated beat signal. The calibration is achieved by recording a series of cross-correlation traces, with one pixel held at ground and the other set to a series of different voltages. The phase response is derived from the temporal shift of the beat signal as a function of applied voltage. No phase change was observed below a threshold voltage of $\simeq$1 V. Above threshold the phase change increases rapidly at first and then more slowly, reaching 2π at 2.5 V and 2.3π at 4.0 V, for example. Our calibration is accurate to approximately $\pm$1.5%.

We have utilized gray-level control of the optical phase to achieve femtosecond pulse-position modulation. We rely on the fact that if $f(t)$ and $F(\omega)$ are a Fourier-transform pair, then the delayed signal $f(t-\tau)$ is the Fourier transform of $F(\omega)\exp(-i\omega\tau)$. Thus a pulse can be retarded (or advanced) by imposing a linear phase sweep onto its spectrum. The delay τ is given by the relation $\tau = \delta\phi/2\pi\delta f$, where $\delta\phi$ and δf are, respectively, the imposed phase change per pixel and the change in optical frequency from one pixel to the next. For our setup δf is approximately 0.230 THz, and therefore $\tau \simeq 4.34(\delta\phi/2\pi)$ psec. Figure 3(a) shows cross-correlation traces of the pulses emerging from the shaper for several values of $\delta\phi$. These data were obtained by using a computer-interfaced driver circuit that independently controlled the voltages applied to each of the 32 modulator pixels. For $\delta\phi = 0$, the pulse arrives at $t = 0$. For the other traces, corresponding to $\delta\phi = \pm0.14\pi$ and $\pm0.25\pi$, the pulse is shifted over a range many times the pulse duration. The pulse arrival times are consistent with the simple formula given above.

Although the pulse-position modulation works nicely over a moderate range of delays, for $|\tau| > 0.5$ psec a loss of peak intensity, an increase in the energy in the wings, and a slight pulse broadening become apparent. In the current experiments, in which $\delta\phi \ll \pi$, these distortions arise mainly owing to the 5-μm gaps separating the electrodes. Because the gap regions sense only the fringing fields associated with the neighboring electrodes, the phases in these regions are not properly controlled, and this induces a significant

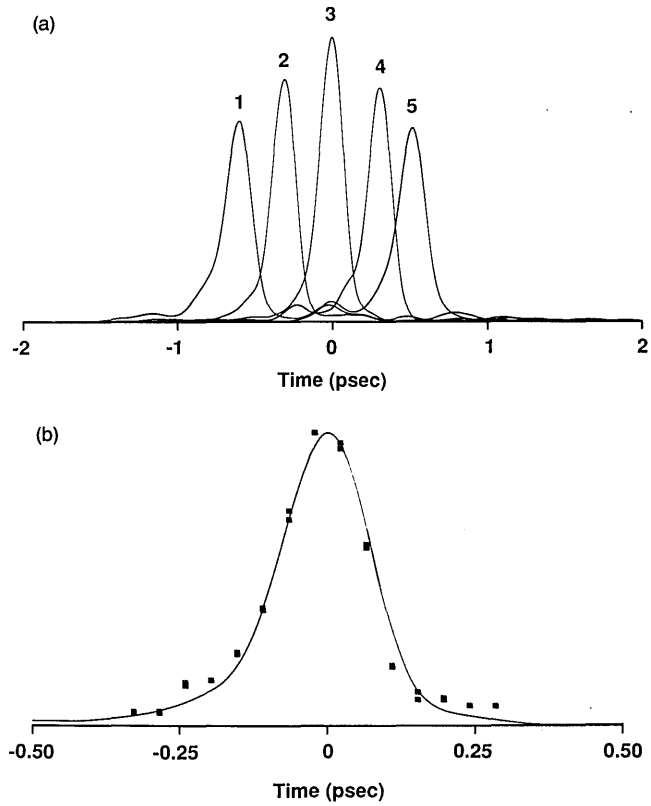

Fig. 3. (a) Intensity profiles of temporally shifted pulses measured by cross correlation with 75-fsec pulses directly from the colliding-pulse mode-locked laser. The changes in phase ($\delta\phi$) from one modulator element to the next are curve 1, -0.25π; curve 2, -0.14π; curve 3, 0; curve 4, 0.14π; curve 5, 0.25π. (b) Comparison of the cross-correlation measurement obtained by using a stepper-motor-driven translation stage to increment the delay (the solid curve) and a cross-correlation measurement obtained with no moving parts by means of the multielement phase modulator (the squares).

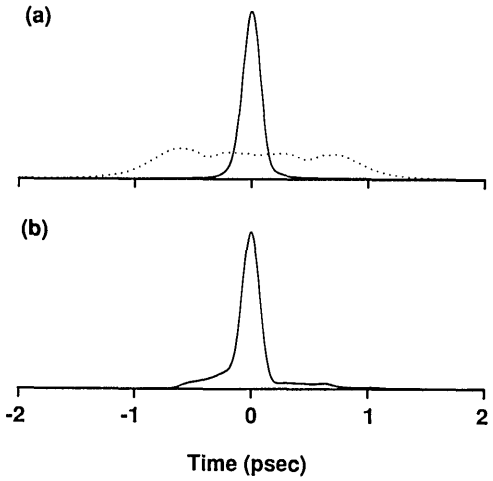

Fig. 4. (a) Cross-correlation traces of pulses obtained with the gratings at their normal positions (the solid curve) and with one of the gratings moved 2.3 cm closer to the lens pair (the dotted curve). (b) Cross-correlation trace of a compressed pulse that results when the appropriate quadratic phase shift is applied by the multielement modulator.

amount of scattering loss. These effects can be minimized by reducing the size of the gaps in future designs.

We can use pulse-position modulation to perform cross-correlation measurements without moving parts. This is illustrated by Fig. 3(b), which compares a cross correlation obtained when the delay is varied by use of a stepper-motor-driven translation stage (the solid curve) with a measurement obtained by use of the multielement modulator to vary the delay with the stage fixed (the squares). In the latter case the delay was sequentially varied over a 600-fsec range by a series of discrete steps. Each step corresponds to a change in $\delta\phi$ by 0.02π and a delay increment of 44 fsec. The excellent agreement between the two measurements gives further indication of the fidelity of our pulse-position modulation technique.

We have also used our gray-level phase control to achieve programmable compression of chirped pulses. In the spectral domain, linearly chirped pulses exhibit a phase response that varies quadratically with frequency. By use of the multielement modulator to compensate for the quadratic phase shift, linearly chirped pulses can be compressed down to the bandwidth limit. We demonstrated this point by moving one of the gratings in the pulse shaper closer to the lens pair. This introduces temporal dispersion,[13] which results in a chirped and broadened output pulse. Cross correlations of pulses obtained with the gratings at their normal positions and with one of gratings moved 2.3 cm are shown in Fig. 4(a). The output pulse is broadened by >10 times to $\simeq$1.9 psec, and the intensity is correspondingly reduced. Figure 4(b) shows the compressed pulse obtained when the appropriate quadratic phase shift is applied by the modulator. The duration is identical to that of the original pulse, and distortion is minimal. Our technique holds out the possibility of compensating for cubic and higher-order phase variations, which arise, for example, in pulse compression below 10 fsec.[1]

In summary, we have described a high-resolution, programmable pulse-shaping apparatus with which we have demonstrated femtosecond pulse-position modulation and programmable femtosecond pulse compression. We expect programmable pulse shaping to become a powerful tool for ultrafast spectroscopy and nonlinear optics and for optical communications based on spectral manipulation of ultrashort pulses.

We thank Meir Orenstein for contributions to the design of the driver circuit and Luis Carrion for its construction.

References

1. R. L. Fork, C. H. Brito Cruz, P. C. Becker, and C. V. Shank, Opt. Lett. **12,** 483 (1987).
2. C. Froehly, B. Colombeau, and M. Vampouille, in *Progress in Optics,* E. Wolf, ed. (North-Holland, Amsterdam, 1983), Vol. 10, pp. 115–121.
3. J. P. Heritage, A. M. Weiner, and R. N. Thurston, Opt. Lett. **10,** 609 (1985).
4. A. M. Weiner, J. P. Heritage, and J. A. Salehi, Opt. Lett. **13,** 300 (1988); A. M. Weiner, J. P. Heritage, and E. M. Kirschner, J. Opt. Soc. Am. B **5,** 1563 (1988).
5. M. Haner and W. S. Warren, Opt. Lett. **12,** 398 (1987); Appl. Phys. Lett. **52,** 1458 (1988).
6. T. Kobayashi and A. Morimoto, in *OSA Proceedings on Picosecond Electronics and Optoelectronics,* T. C. L. G. Sollner and D. M. Bloom, eds. (Optical Society of America, Washington, D.C., 1989), p. 81.
7. A. M. Weiner, J. P. Heritage, R. J. Hawkins, R. N. Thurston, E. M. Kirschner, D. E. Leaird, and W. J. Tomlinson, Phys. Rev. Lett. **61,** 2445 (1988).
8. W. S. Warren, Science **242,** 878 (1988).
9. A. M. Weiner, Y. Silberberg, H. Fouckhardt, D. E. Leaird, M. A. Saifi, M. J. Andrejco, and P. W. Smith, IEEE J. Quantum Electron. **25,** 2648 (1989).
10. A. M. Weiner, D. E. Leaird, G. P. Wiederrecht, and K. A. Nelson, "Femtosecond pulse sequences used for optical manipulation of molecular motion," Science (to be published).
11. J. A. Valdmanis, R. L. Fork, and J. P. Gordon, Opt. Lett. **10,** 131 (1985).
12. P. G. de Gennes, *Physics of Liquid Crystals* (Oxford U. Press, Oxford, UK, 1974).
13. O. E. Martinez, IEEE J. Quantum Electron. **QE-23,** 59 (1987).